Giant Hall effect in Ni-Mn-In Heusler alloys

I. Dubenko, A. K. Pathak, S. Stadler,* and N. Ali
Department of Physics, Southern Illinois University, Carbondale, Illinois 62901, USA

Ya. Kovarskii, V. N. Prudnikov, N. S. Perov, and A. B. Granovsky
Department of Physics, M.V. Lomonosov Moscow State University, Moscow 119991, Russia

(Received 24 March 2009; revised manuscript received 12 August 2009; published 28 September 2009)

We present experimental results on the giant Hall effect in the Heusler alloy $Ni_{50}Mn_{50-x}In_x$ with $x=15.2$. An unusual field dependence of the Hall resistivity (ρ_H) was observed in the vicinity of the martensitic phase transition, where ρ_H sharply increases up to ρ_H (15 kOe)=50 $\mu\Omega$ cm. This value is comparable with the giant Hall resistivity in magnetic nanogranular alloys. Associated with ρ_H, the Hall angle reaches a giant value of $\tan^{-1}$ 0.5. An explanation of the giant Hall effect in $Ni_{50}Mn_{50-x}In_x$ Heusler alloys has been suggested.

DOI: 10.1103/PhysRevB.80.092408 PACS number(s): 75.30.Kz, 73.50.Jt, 72.20.My, 72.80.Ga

Since the observation the Hall effect in ferromagnetic materials in 1879, and especially its spontaneous counterpart, the anomalous Hall effect (AHE), it has been a subject of intense theoretical and experimental interest (for reviews see Refs. 1–4, and references therein). The Hall resistivity $\rho_H(\rho_{xy})$ in ferromagnets can be written as a sum of two terms

$$\rho_{xy} = \rho_H = R_0 B_z + R_s 4\pi M_z, \quad (1)$$

where the first term describes the ordinary Hall effect, which is related to the Lorentz force, and the second one is the AHE resistivity where R_s is the AHE coefficient, and M_z and B_z are magnetization and magnetic induction components, respectively. It is well established that the AHE originates from spin-orbit interactions, but the main mechanisms of the AHE are still under debate, and some experimental results are still unexplained (see, for examples, Refs. 5–7). Besides the practical importance of the AHE for spintronics applications and magnetic sensing, this effect can provide unique information about the electronic band and ionic structures, phase transitions, spin polarization of current carriers, and so on. In addition, many other phenomena, such as anomalous thermomagnetic effects such as the Nernst-Ettingshausen effect, the spin Hall effect, the optical Hall effect, and the magneto-optical properties in the infrared band have the same origin.[3]

The most puzzling, and still far from being well understood, behavior of the AHE was found in heterogeneous magnetic nanogranular alloys with a metal volume fraction close to the percolation threshold.[5] Such systems exhibit a giant AHE (GHE) with the magnitude of R_s at least three orders larger than that for Ni or Fe without any $R_s \sim \rho^2$ or $R_s \sim \rho$ correlations. It was found that the GHE appears only if the composition of these heterogeneous systems is very close to the percolation threshold, and if the granular size is less than several nanometers. Several hypotheses, such as enhanced spin-orbit interaction,[8] enhanced scattering by interfaces,[9] and quantum percolation[10] were proposed, but each of these hypotheses has its own drawback.

A strong magnetic and structural heterogeneity as observed in nanogranular alloys can be expected in off-stoichiometric Ni-Mn-In Heusler alloys. Some of these compounds demonstrate a temperature-induced first-order structural phase transition from a high-temperature austenitic phase (cubic $L2_1$ or B2 crystal structure) to a low-temperature martensitic phase at T_M (or reverse transition at T_A) characterized by a crystal cell of lower symmetry.[11] The properties of the alloys are strongly influenced by magnetic field, temperature, composition, mechanical stresses, and treatment prehistory. As a result, the alloys exhibit a magnetic field-induced reverse martensitic transition from the low magnetization martensite to the higher magnetization austenite at $H=H_M$, exchange bias, giant magnetocaloric effects, nonreciprocal effects in magnetization, and so on (see Refs. 12–15).

In this Brief Report we will focus on the alloy $Ni_{50}Mn_{50-x}In_x$ with $x=15.2$ as the typical representative sample of $Ni_{50}Mn_{50-x}In_x$ system. We report the experimental results on the Hall resistivity, ρ_H (H,T). We observed very unusual field dependences of ρ_H (H,T), no correlation between AHE and ordinary resistivity ρ, and a giant value of Hall effect angle, $\theta_H=\tan^{-1}(\rho_H/\rho)=\tan^{-1}$ 0.5. All of these features are due to the strong disorder and clusterlike microstructure of the alloy.

The sample has been fabricated using the conventional arc-melting method described in detail in Ref. 15. The magnetic measurements at low magnetic fields and fields up to 15 kOe were made using a vibrating sample magnetometer (VSM, LakeShore 7400 System), and fields up to 50 kOe fields by a superconducting quantum interference device magnetometer (Quantum Design). Magnetotransport measurements were carried out using the standard four-point method using a fully automated system in a temperature interval 77–400 K at magnetic fields (H) in the range 5–15 000 Oe. Temperature-dependent magnetization curves ($M(T)$) were measured in $H=0.2$ and 50 kOe fields, and in the temperature range 5–400 K. The transition temperatures have been determined using the local maxima of dM/dT curves. Magnetization measurements were carried out during heating after the sample was cooled from 400 to 5 K at $H=0$ [zero field cooled (ZFC)], if it is not specifically stated otherwise.

The $M(T)$ curves for $Ni_{50}Mn_{34.8}In_{15.2}$ [see Fig. 1(a)] are characterized by sharp changes in magnetization at $T_{M,A}$ and at the Curie temperature (T_C), hysteresis of $M(T)$, and a strong shift of $T_{M,A}$ to low temperatures with increasing magnetic field. The magnetization isotherms [see Fig. 1(b)] are

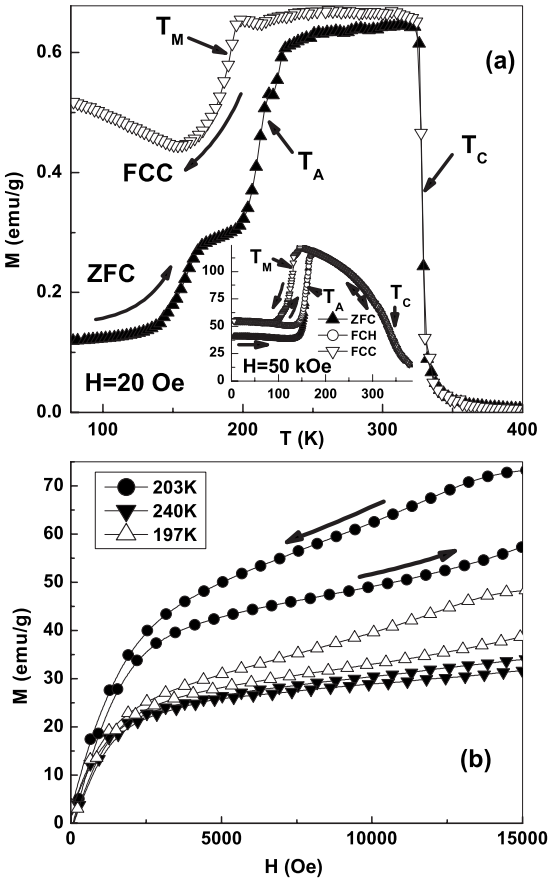

FIG. 1. The distinctive magnetic properties of $Ni_{50}Mn_{34.8}In_{15.2}$: (a) $M(T)$ curves obtained with $H=20$ Oe and 50 kOe (inset). $M(T)$ curves were carried out during the cooling process (from 400 K) in the presence of magnetic field [field cooled cooling (FCC)], and while heating after the sample was cooled from 400 to 5 K in the presence of magnetic field [field cooled heating (FCH)]. (b) Magnetization isotherms at different temperatures. Arrows indicate the transition temperatures and the directions of the temperature (a) or magnetic field (b) changes during the measurements.

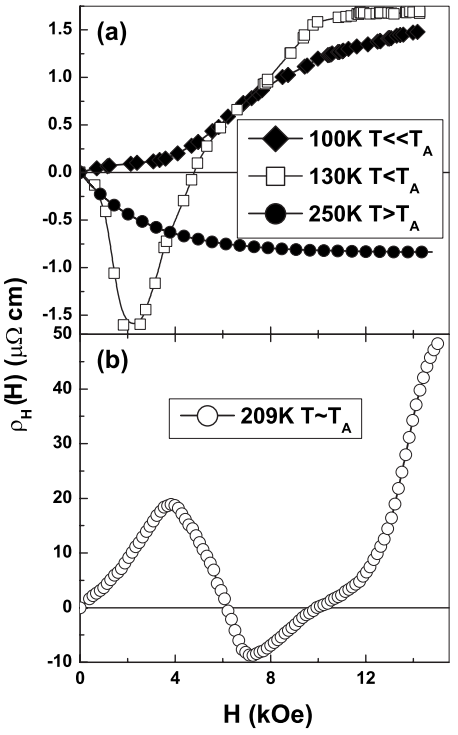

FIG. 2. [(a) and (b)] Hall resistivity of $Ni_{50}Mn_{34.8}In_{15.2}$ at different temperatures.

not saturated even at 15 kOe at $T<T_A$, and exhibit the behavior associated with a field-induced martensitic metamagnetic transition in the vicinity of $T_{M,A}$ [see $M(H)$ at $T=197$ and 203 K in Fig. 1(b), and Ref. 12].

The obtained results for the dependences of the ρ_H on magnetic field and temperature are presented in Fig. 2. If $T>T_A$ [Fig. 2(a)], ρ_H increases with applied field and the curve changes its slope at some field because the second term in Eq. (1), corresponding to the AHE, tends to saturate with magnetization, but the first term continues to grow with magnetic field. This is a typical behavior for ρ_H of most common magnetic materials. However, when $T<T_A$, Fig. 2 shows abnormal field dependences. More specifically, $\rho_H(H)$ does not tend to saturate even at 15 kOe; its slope changes once (or even twice), and sometimes changes sign. Moreover, in the vicinity of T_A, $\rho_H(H=15$ kOe) reaches a very large value of 50 $\mu\Omega$ cm, which is about two to three orders of magnitude greater than that observed at this temperature for any common magnetic materials.[1,2] This value is only four times smaller than the GHE in all-magnetic nanogranular alloys NiFe-SiO_2 with compositions close to the percolation threshold,[5] and it is at least five times greater than the AHE observed for metallic, high-resistivity nanogranular alloys.[6,7] However, the $Ni_{50}Mn_{38.4}In_{15.2}$ compound has a much smaller ordinary resistivity compared to nanogranular alloys, and therefore the Hall angle $\theta_H=\tan^{-1}(\rho_H/\rho)$ reaches a giant value of $\theta_H=\tan^{-1}(0.5)$.

We will now make a qualitative explanation that is self-consistent with the data, by considering that the alloy is composed of two components: the first one is in the austenitic phase with a volume fraction c, and the second one is in the martensitic phase with volume fraction $1-c$. The key point is that the GHE can be observed only in the case where nanosized granules of ferromagnetic (FM) metal form a percolation network in a matrix. We can reasonably assume that, when T close below T_A, nanosized grains or clusters of austenitic phase are dispersed in the martensitic matrix with a concentration close to the percolation threshold. Therefore we can estimate the volume fraction of austenitic phase at T_A as the percolation threshold of the mixture of spherical balls $c(T_A)=0.33$. This value is quite reasonable because, at room temperature which is about 90 K above T_A, x-ray diffraction (XRD) experiments give $1-c$ as about 14%.[15] Since the matrix is a metal, the resistivity of $Ni_{50}Mn_{34.8}In_{15.2}$ is much smaller than in the case of NiFe-SiO_2. Because the austenitic grains are of nanosize, they can be of single domain or superparamagnetic (SP). There is no saturation of either the magnetization or the Hall effect resistivity in $H=15$ kOe, hence it is possible to conclude that, at $T<T_A$ and in $H<H_M$, the austenitic grains are in a superparamagnetic state. Thus, in certain temperature interval below T_A and $H<H_M$, there is a small amount of SP grains in a FM matrix, and

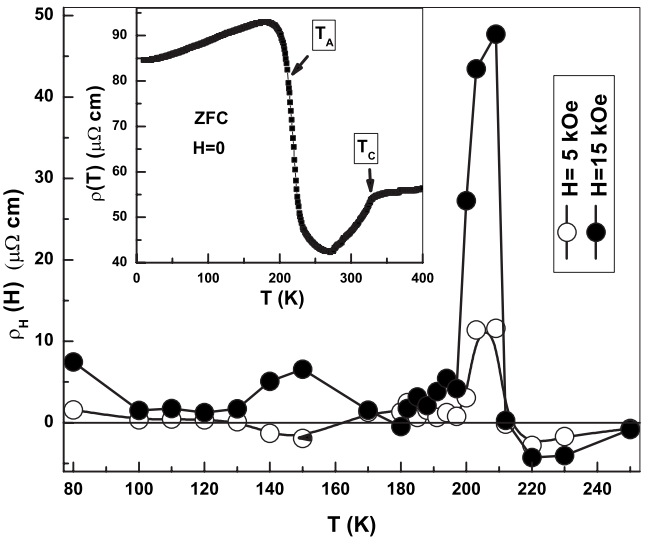

FIG. 3. Temperature dependencies of ρ_H for $Ni_{50}Mn_{34.8}In_{15.2}$ at 5 and 15 kOe. Inset: temperature dependence of $\rho(T)$ of $Ni_{50}Mn_{34.8}In_{15.2}$ at $H=0$.

each of these grains play the role of a nucleus of austenitic phase and are responsible for the irreversibility in the system. (The significant amount of austenitic fraction has been reported in Ref. 16 far below T_M from direct XRD measurements in a $Ni_2Mn_{1.4}Sb_{0.6}$ alloy showing similar behavior to that of $Ni_{50}Mn_{34.8}In_{15.2}$.) With increasing temperature, the volume fraction of these grains increases and therefore the magnetization gradually decreases. At T_A they form a percolation network and become ferromagnetic and, as a result the magnetization sharply increases. Both the size and the amount of austenitic grains increase with magnetic field, resulting in a shift of T_A to low temperature, and a field-induced metamagnetic transition (Fig. 1).

In the framework of the effective-medium theory, the Hall resistivity of a two-component system can be written as follows:[17]

$$\rho_H = \frac{1-c}{(1-c)+c\left(\frac{\rho_2}{\rho_1}\right)^2\left(\frac{\rho+2\rho_1}{\rho+2\rho_2}\right)^2}[R_{01}B_{z1}+4\pi R_{s1}M_{z1}]\left(\frac{\rho}{\rho_1}\right)^2 + \frac{c}{c+(1-c)\left(\frac{\rho_2}{\rho_1}\right)^2\left(\frac{\rho+2\rho_1}{\rho+2\rho_2}\right)^2}[R_{02}B_{z2}+4\pi R_{s2}M_{z2}] \times\left(\frac{\rho}{\rho_2}\right)^2, \quad (2)$$

where indexes 1 and 2 correspond to the first and second components. The field dependences of the Hall resistivity of the austenitic grains and the martensitic phase are completely different (Fig. 2). It should also be taken into account that the ordinary resistivities of the components are different (inset in Fig. 3) and the system exhibits magnetoresistance. As a result, according to Eq. (2), there is a very complicated field dependence of the total Hall resistivity (Fig. 2), which is not a simple sum of Hall resistivities of the martensitic and austenitic phases, and there is no correlation between ρ_H and ρ.

Let us come back to the main result of the present work—the observation of the GHE and the GHE angle. Since the system under consideration is metallic, we can exclude the presence of several mechanisms, such as quantum percolation[10] or the influence of high-resistivity contacts between grains.[9] It should be emphasized that the increase in the AHE near $T_{M,A}$ is accompanied by a decrease in the resistivity (see inset in Fig. 3 at T_A). It means that interface scattering and size effects (both quasiclassical and quantum) are not responsible for the observed behavior, and that different groups of current carriers are responsible for the AHE and resistivity. Indeed, the AHE originates from spin-orbit interactions that are strong for *d*-like electrons but weak for *s*-like electrons.

To proceed further, four features should be pointed out. (i) The GHE was observed only for fields corresponding to metamagnetic behavior. (ii) The GHE takes place only in a very narrow interval of temperatures, and ρ_H changes its sign immediately after reaching the maximum value. (iii) The ρ_H does not tend to saturate at 15 kOe. (iv) At the temperature corresponding to the maximum of the Hall resistivity, the diagonal σ_{xx} and off-diagonal σ_{xy} conductivities are of the same order of magnitude.

As far as metamagnetic transitions in metallic systems are associated with electronic band-structure changes, and since the Hall resistivity changes its sign in the vicinity of martensitic transition [see Figs. 2(a) and 2(b)], we can conclude that the main reason for the GHE (while heating) in our case is an electronic band-structure transformation accompanied by an increase in the total density of states at the Fermi level $N(E_F)$, mostly from the *d* component of $N^d(E_F)$, where the Fermi level crosses the degenerate *d* states. The electronic band-structure transformation might occur at T_A, and it is accompanied with appearance of long distance ferromagnetic order of the austenitic phase. Since the $N(E_F)$ is larger for the austenitic phase compared to the martensitic modification of the crystal structure,[18,19] and the ordinary resistivity $\rho = 1/\sigma_{xx} \sim 1/[N(E_F)^2]$, $\rho(T)$ decreases during this transformation (see inset in Fig. 3) in spite of the increase in thermal disorder that confirms the aforementioned statement. But if $\sigma_{xx} \sim A[N(E_F)^2]$, where A depends on the scattering potential ($A \sim V^{-2}$), the off-diagonal conductivity σ_{xy} is much more strongly related to the density of states, and specifically to the *d*-state contribution, $N^d(E_F)$, to the total density of states. The order of magnitude of σ_{xy} can be estimated as[3,4,20,21]

$$\sigma_{xy} \sim \sigma_{xx}^d \frac{\lambda_{so}}{\Delta}\{V[N^d(E_F)]\}^\alpha \sim A\frac{\lambda_{so}}{\Delta}[N^d(E_F)]^2\{V[N^d(E_F)]\}^\alpha, \quad (3)$$

where λ_{so} is the spin-orbit parameter, Δ is the energy difference between two subbands coupled by spin-orbit interaction, V is linearly dependent on the scattering potential, $\alpha = 1$ in the case of skew scattering, and $\alpha = 2$ in the case of side jump or an intrinsic mechanism.[3,4,20,21] As a result, ρ_H and Hall angle can be written as follows:

$$\rho_H = \sigma_{xy}/[(\sigma_{xx})^2 + (\sigma_{xy})^2] \approx \frac{1}{A}\frac{\lambda_{so}}{\Delta}\frac{[N^d(E_F)]^2\{V[N^d(E_F)]\}^\alpha}{[N(E_F)]^4}, \tag{4}$$

$$\theta_H = \tan^{-1}(\rho_H/\rho) \approx \tan^{-1}\left(\frac{\lambda_{so}}{\Delta}\frac{[N^d(E_F)]^2\{V[N^d(E_F)]\}^\alpha}{[N(E_F)]^2}\right). \tag{5}$$

It follows from Eqs. (4) and (5) that the GHE can be observed only when the ratio $\frac{\lambda_{so}}{\Delta}$ is significant. This should be the case if the Fermi level is located in the very narrow interval of energy of degenerate states $\Delta \sim \lambda_{so}$.[21,22] This interval of energy is comparable to $k_B T_{M,A}$. This condition in some sense resembles the idea of enhanced spin-orbit interaction at interfaces.[8] In addition, the scattering should be strong $V(N^d(E_F) \sim 1$, and this is the case because the resistivity is about 100 $\mu\Omega$ cm. The proposed scheme allows us also to explain the increase in Hall resistivity ρ_H simultaneously with the decrease in ordinary resistivity $\rho(T)$ (Fig. 3). That follows from Eq. (4) when $N(E_F)$ increases [due to an increase in $N^d(E_F)$]. The proposed model also explains that the observed value of the GHE angle is quite unique in the sense that several requirements should be satisfied to obtain the value of the angle.

Finally, it should be strongly emphasized here that, regardless of the proposed mechanism of the GHE in Heusler alloys, the giant value of the Hall angle is the most important characteristic for possible applications of the Hall effect in spintronics and magnetic sensors.

This work was supported by the Russian Foundation for Basic Research (Grant No. 09-02-00309) and the Research Corporation (Grant No. RA-0357), and by the Office of Basic Energy Sciences, Material Sciences Division of the U.S. Department of Energy (Contract No. DE-FG02-06ER46291).

*Also at Department of Physics and Astronomy, Louisiana State University, Baton Rouge, LA 70803, USA.

[1] C. M. Hurd, *The Hall Effect in Metals and Alloys* (Plenum, New York, 1972).

[2] *The Hall Effect and its Applications*, edited by C. L. Chien and C. R. Westgate (Plenum, New York, 1979).

[3] A. Vedyaev, A. Granovsky, and O. Kotelnikova, *Transport Phenomena in Disordered Ferromagnetic Alloys* (Moscow State University, Moscow, 1992) (in Russian).

[4] J. Sinova, T. Jungwirth, and J. Cerne, Int. J. Mod. Phys. B **18**, 1083 (2004).

[5] A. B. Pakhomov, X. Yan, and B. Zhao, Appl. Phys. Lett. **67**, 3497 (1995); A. B. Pakhomov and X. Yan, Solid State Commun. **99**, 139 (1996); Physica A **229**, 402 (1996).

[6] J. Gao, F. Wang, X. L. Jiang, G. Ni, F. M. Zhang, and Y. W. Du, J. Appl. Phys. **93**, 1851 (2003).

[7] G. X. Miao and Gang Xiao, Appl. Phys. Lett. **85**, 73 (2004).

[8] J.-Q. Wang and G. Xiao, Phys. Rev. B **51**, 5863 (1995).

[9] A. Granovsky, F. Brouers, A. Kalitsov, and M. Chshiev, J. Magn. Magn. Mater. **166**, 193 (1997).

[10] C. Wan and P. Sheng, Phys. Rev. B **66**, 075309 (2002).

[11] T. Krenke, E. Duman, M. Acet, E. F. Wassermann, X. Moya, L. Mañosa, A. Planes, E. Suard, and B. Ouladdiaf, Phys. Rev. B **75**, 104414 (2007).

[12] V. K. Sharma, M. K. Chattopadhyay, and S. B. Roy, Phys. Rev. B **76**, 140401(R) (2007).

[13] I. Dubenko, M. Khan, A. K. Pathak, Bhoj Raj Gautam, Shane Stadler, and Naushad Ali, J. Magn. Magn. Mater. **321**, 754 (2009).

[14] A. K. Pathak, G. Bhoj, M. Khan, I. Dubenko, S. Stadler, and N. Ali, J. Appl. Phys. **103**, 07F315 (2008).

[15] A. K. Pathak, M. Khan, B. R. Gautam, S. Stadler, I. Dubenko, and N. Ali, J. Magn. Magn. Mater. **321**, 963 (2009).

[16] S. Chatterjee, S. Giri, S, Majumdar, A. K. Deb, S. K. De, and V. Hardy, J. Phys.: Condens. Matter **19**, 346213 (2007).

[17] A. Granovsky, A. Vedyaev, and F. Brouers, J. Magn. Magn. Mater. **136**, 229 (1994).

[18] P. J. Brown, A. Y. Bargawi, J. Crangle, K.-U. Neumann, and K. R. A. Ziebeck, J. Phys.: Condens. Matter **11**, 4715 (1999).

[19] S. Fujii, S. Ishida, and S. Asano, J. Phys. Soc. Jpn. **58**, 3657 (1989).

[20] J. M. Luttinger, Phys. Rev. **112**, 739 (1958).

[21] S. Onoda, N. Sugimoto, and N. Nagaosa, Phys. Rev. Lett. **97**, 126602 (2006).

[22] S. Onoda, N. Sugimoto, and N. Nagaosa, Phys. Rev. B **77**, 165103 (2008).